IEEE Access
Multidisciplinary | Rapid Review | Open Access Journal

Received January 8, 2020, accepted January 26, 2020, date of publication January 29, 2020, date of current version February 6, 2020.

Digital Object Identifier 10.1109/ACCESS.2020.2970191

Multiple Access Noise Compensation in CO-OFDMA-PON Uplink Transmission Using Digital Phase Conjugated-Pilot Tones

SOO-MIN KANG, HYOUNG JOON PARK, INHO HA, AND SANG-KOOK HAN, (Senior Member, IEEE)
Department of Electrical and Electronic Engineering, Yonsei University, Seoul 03722, South Korea

Corresponding author: Sang-Kook Han (skhan@yonsei.ac.kr)

This work was supported by the National Research Foundation of Korea (NRF) grant funded by the Korean Government, Ministry of Science and ICT (MSIT), under Grant 2019R1A2C3007934.

ABSTRACT In coherent orthogonal frequency division multiple accessing technique-based passive optical network (CO-OFDMA-PON) uplink transmission, two main multiple-access noises (MNs), which are multiple- state-of-polarization leakages (SOPLs) and phase noises (PNs) inevitably occur by various optical network units (ONUs) and interfere with the uplink signal in this system. These MNs are different by optical devices and paths of each ONU. In this regard, parallel MNs handling per ONU is necessary to provide uplink service. We propose digital phase conjugated pilot-tones (DPC-PTs) based MNs compensation technique. This can deal with MNs by using superposition of two adjacent pilot subcarriers. In the experiments conducted, we applied a pair of DPC-PTs per ONU to handle two MNs and performed parallel processing for each ONU. The transmission performance in terms of root-mean-square error, error-vector magnitude, bit-error-rate (BER), and the overhead of redundant PTs was improved by using the proposed technique in 20-km CO-OFDMA-PON uplink transmission. Both MNs were effectively compensated by comparing transmitted and received DPC-PTs. Minimum overhead of 0.39 % OFDMA symbol duration was verified to meet BER target in the given transmission condition. It guarantees more accurate tracking of SOPL than single-PT-based one due to the doubled number of estimator samples. Besides, more accurate tracking of PNs is demonstrated due to lower noise level between DPC-PTs. As a result, applicability to the phase and polarization diversities-based coherent multiple access is demonstrated through the proposed MNs tracking technique.

INDEX TERMS Coherent optical communications, phase noise, polarization, multiple access, passive optical network.

I. INTRODUCTION

In the future passive optical network (PON), sufficient receiver sensitivity has been required to support both massive subscribers and long-reach transmission [1]. Besides, exponentially increased demand for data-rate is required to provide various service signals such as fifth generation service.

The most common network solution in the PON system is an intensity modulation-based direct detection PON (IM/DD PON). In this system, an electrical signal is directly modulated to the semiconductor laser sources or optical external modulators. Then, the modulated signal can be received by using the photodetector (PD) at the receiver part. It converts the received optical signal into the electrical signal by the square-law detection principles. To go near to both high data-rate and long-reach target, multi-carrier-based PON such as orthogonal frequency division multiplexing PON (OFDM-PON) has been proposed by overlapping subcarriers to increase the spectral efficiency (SE) [2]. Otherwise, polarization division multiplexing PON (PDM-PON) can also be used to double SE in the given signal-to-noise ratio (SNR) condition [3]. Both OFDM and PDM solutions ensure spectral efficient system within the single wavelength. However, it is hard to follow up network requirements; e.g., SE is restricted

The associate editor coordinating the review of this manuscript and approving it for publication was San-Liang Lee.

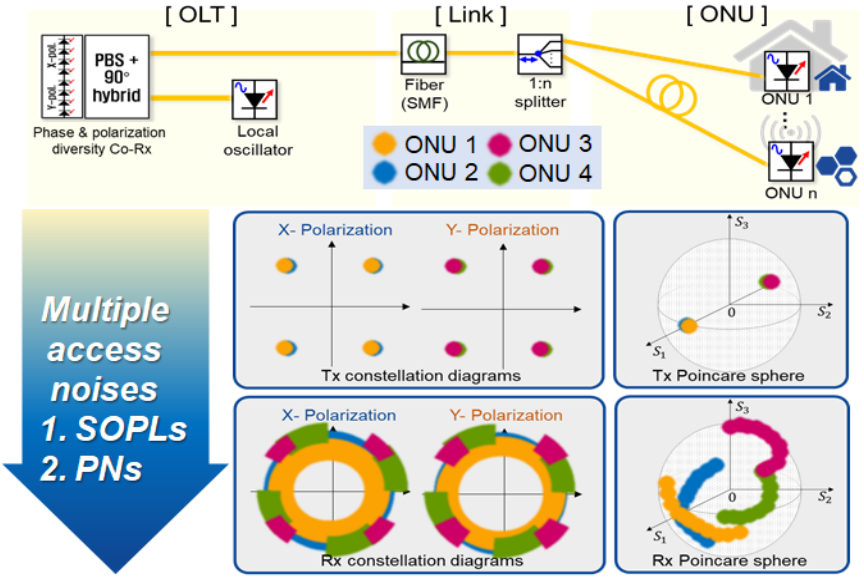

FIGURE 1. Multiple access noises in CO-OFDMA-PON.

because only optical intensity can be modulated. Above all, the sensitivity of the direct detection-based receiver side is limited, so it is not adequate for long-reach transmission or high-order modulation-based systems. To overcome the low receiver sensitivity, several wavelength resources-based transmission techniques have been proposed to remarkably expand the total data-rate [4], [5]. However, these wavelength division multiplexing techniques can give us the burden of both system complexity and stabilization.

As an attractive network solution of IM/DD PON, a coherent PON (CO-PON) system makes it possible to receive optical field-modulated signals with sufficient receiver sensitivity [6], [7]. CO-PON uses optical beating gain from a local oscillator (LO) at the receiver side, as a result, even better receiver sensitivity can be strongly appealed for massive subscribers, long transmission reach. Additionally, optical field index such as intensity, phase, polarization can be modulated and demodulated because the coherent receiver can detect these optical field diversities. So, high data capacity requirements can be ensured. That is, a desirable system setup for future PON can be realized. If a multi-carrier system such as an OFDM or advanced version of OFDM in [8], [9] is applied to CO-PON, spectral efficiency can be maximized by orthogonally overlapping each subcarrier and allocating bits dynamically. Moreover, if multiple optical network units (ONUs) are accessed with orthogonal frequency division multiple-access (OFDMA), which means that each OFDMA frame of n-numbers of ONUs is transmitted at the same time, flexible resource management including frequency and power can be employed [9]. When both phase and polarization diversity-based coherent receiver is installed in CO-OFDMA-PON, the scalability for PDM can double data capacity within given single wavelength [10].

Figure 1 depicts the optical phase and polarization issues in CO-OFDMA-PON uplink transmission. Herein, both diversities-based coherent receiver is used, where both optical hybrid structure and polarization beam splitters are integrated into the receiver for the scalability to PDM-CO-OFDMA-PON. Let's assume that uplink signal components of *4*-numbers of ONUs with 4 quadrature/amplitude modulation (4QAM) are multiple-accessed in dual-polarization axes as depicted in the constellation diagram and Poincare sphere representation at Fig. 1. However, both diagrams cannot be maintained in the practical environment of multiple-access owing to the various multiple-access noises (MNs) [11]–[13]. MNs mean noise components from n-number of ONUs when multiple ONUs are simultaneously accessed to optical line terminal (OLT): i.e., noise components at *n-to-1* multiple access. Among various MNs as mentioned in [11]–[13], in this paper, we focus on two main MNs: multiple state-of-polarization leakages (SOPLs) and phase noises (PNs) among n-numbers of ONUs.

Multiple SOPLs comes from polarization-sensitive optical devices and standard single-mode fiber (SSMF) insertion [11], [12]. Generally, optical devices such as semiconductor-based laser sources, external modulators, amplifiers, and attenuators have polarization-sensitivities. In addition, in SSMF, SOP can be changed randomly due to birefringence property and external changes such as temperature, pressure, and physical bending can vary SOP also. As a result, the SNR at the desired axis is degraded as shown in Fig. 1. This issue gets worse when both the number of polarization-sensitive devices and transmission distance are increased. Further, when the transmission situation is extended to PDM, polarization crosstalk components between two orthogonal axes can be generated as shown

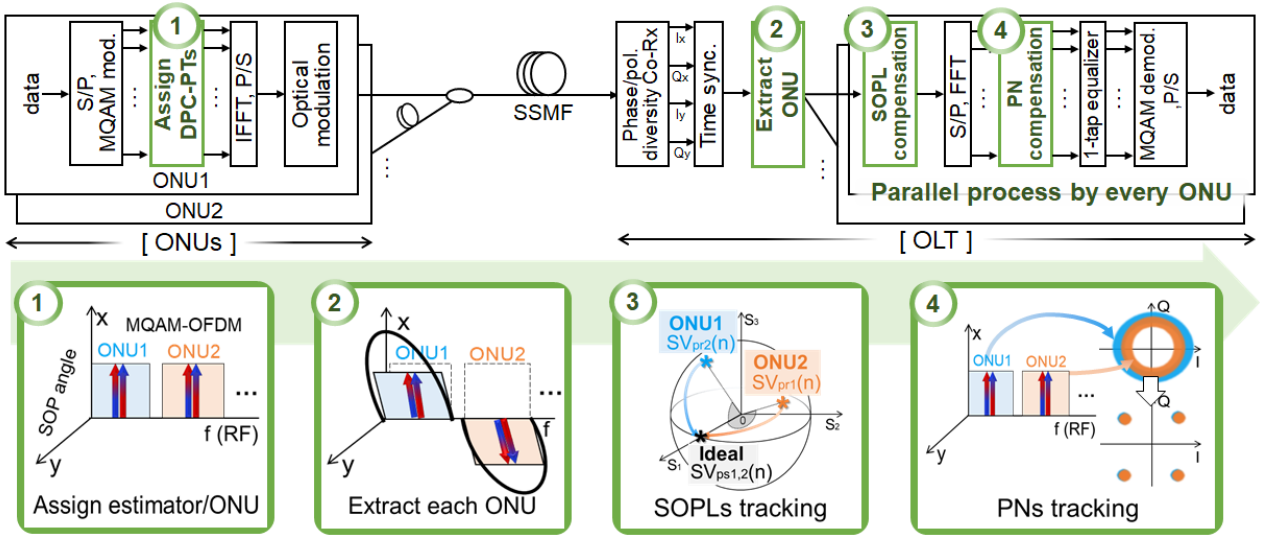

FIGURE 2. Proposed DPC-PTs based multiple access noise compensation in CO-OFDMA-PON uplink transmission.

in Fig. 1. On the other hand, multiple PNs are caused by the unstable temperature/current control of both lasers of source and LO [13], [14]. They cause both common phase error (CPE) and inter-channel interference (ICI) components. The CPE rotates the transmitted symbol and the ICI increases the noise floor as depicted in Fig. 1. They also degrade the transmission performance and become more severe if a wider laser linewidth, higher modulation order, and narrower OFDM subcarrier spacing are used. It is worthy of note that the effects of the two MNs can differ in each ONU because each ONU has different optical devices and optical path lengths. This is because it is difficult to match all optical components and path lengths among multiple ONUs in a practical transmission system. Therefore, independent handling per ONU is necessary to ensure two MNs mitigation.

Recently, many research groups including our research groups have suggested a solution for two MNs. To deal with multiple SOPLs, [11] explored optical intensity reception in both polarization axes; however, the modulation format was restricted to intensity modulation. Further, in [12], single pilot-tone (PT)-based independent SOP tracking was proposed without any optical handling of the SOP such as [15], [16]. This technique enabled simpler and faster compensation compared with other complex sample-by-sample tracking methods [17], [18] and transparent for modulation format, whereas tracking accuracy could be degraded in more severe SOPLs owing to the insufficient estimator samples. For the multiple PNs solution, a special differential signaling technique was developed in [13], where the multiple PNs were automatically canceled out during the differential demodulation process. It required no additional phase-locked loop, which could increase the system complexity unlike [19]. Also, the burden of an additional digital filter or overhead due to pilot-symbols with wastage of net data-rate was not required as in [20]. However, only differential-type modulation could be applied and the SNR penalty for differential processing existed [21].

This paper proposes digital phase conjugated pilot-tones (DPC-PTs)-based MNs compensation in the conventional M-ary QAM-based CO-OFDMA-PON uplink transmission. The main contribution is to track both MNs 1) by ONU in parallel and 2) by using the same estimators. In the experiment conducted, a pair of DPC-PTs per ONU-based independent compensation technique was performed in the given transmission condition. Performance improvement in terms of root-mean-square error (RMSE), error vector magnitude (EVM), bit-error-rate (BER), and required overhead was experimentally verified.

II. PROPOSED MULTIPLE ACCESS NOISE COMPENSATION TECHNIQUE

Figure 2 shows the basic principle of the proposed tracking technique. The proposed technique targets to track both MNs in parallel per multiple-accessed ONUs with the same DPC-PTs because each ONU suffers different MNs during transmission. It consists of the following four steps: 1) MN estimator assignment per ONU, 2) ONU extraction for parallel processing, 3) SOPL tracking, and 4) PN tracking. The first step is performed at the transmitter digital signal processing (DSP), while the remaining steps are performed at the receiver DSP. Each received ONU signal is separated in step 2) and remained steps 3) and 4) are performed by the same estimator within unit ONU. A detailed explanation of each step is as bellows.

In the first step, the digital phase conjugated data components are assigned to two adjacent subcarriers by each ONU, which refer to as DPC-PTs. Let us define that the index of the OFDMA frame is defined as $1, \ldots n, \ldots, N$, where the total number of the OFDMA frame is N. We can also define OFDMA subcarrier index as $1, \ldots k, \ldots, K$ when K-number

of subcarrier is used within an ONU. Among K numbers of subcarriers, assume that k- and $(k+1)$-*th* subcarriers are assigned as a pair of DPC-PTs. When a pilot signal is assigned to the k-*th* subcarrier, the digital phase conjugation of this signal is assigned to $(k+1)$-*th* subcarrier. These two subcarriers are defined as a pair of DPC-PTs in this paper. If a pair of DPC-PTs is used, transmitted n-*th* frame of DPC-PTs can be expressed as:

$$\begin{aligned} S_{n,k} &= \left[E_{x_{n,k}};\quad E_{y_{n,k}}\right] = \left[A_x \exp(j\theta_{x_0});\quad A_y \exp(j\theta_{y_0})\right], \\ S_{n,k+1} &= S^*_{n,k} = \left[A_x \exp(-j\theta_{x_0});\quad A_y \exp(-j\theta_{y_0})\right], \end{aligned} \tag{1}$$

where $(*)$, $E_{x_{n,k}}$, $E_{y_{n,k}}$, A_x, A_y, θ_{x_0}, and θ_{y_0} denote phase conjugation, MQAM data components, amplitudes of both x- and y- polarization axes, and the initial phase of the laser, respectively. After performing inverse fast Fourier transform (IFFT), MQAM-OFDMA signal with DPC-PTs per ONU can be generated. Then, each signal component is modulated at the optical modulation block by using an optical external modulator as depicted in Fig. 2. Two modulated signal components are combined by using optical combiner and transmitted to the fiber link. In the next step, after coherent detection and time synchronization, each ONU signal can be extracted by using finite impulse response-based digital band-pass filters for ONU extraction. It is for the parallel MNs compensation per ONU. Remaining steps of 3rd and 4th, MNs per each ONU are tracked and compensated in parallel because of different per ONU. Received DPC-PTs in the n-*th* frame of each ONU can be written as:

$$\begin{aligned} R_{n,k} &= M_p(n) \cdot (CPE_{n,k} \cdot S_{n,k} + major - ICI_{n,k}), \\ R_{n,k+1} &= M_p(n) \cdot (CPE_{n,k+1} \cdot S^*_{n,k} + major - ICI_{n,k+1}). \end{aligned} \tag{2}$$

In (2), $M_p(n)$ is SOP variation matrix during fiber transmission of the n-*th* frame [12], which can be written as:

$$M_p(n) = \begin{bmatrix} \cos(\alpha(n)) \exp(\frac{-j\Delta\beta(n)}{2}) & -\sin(\alpha(n)) \exp(\frac{-j\Delta\beta(n)}{2}) \\ \sin(\alpha(n)) \exp(\frac{j\Delta\beta(n)}{2}) & \cos(\alpha(n)) \exp(\frac{j\Delta\beta(n)}{2}) \end{bmatrix}, \tag{2-1}$$

which consisted of Stokes Vectors (SVs) when $\alpha(n)$ and $\Delta\beta(n)$ are $0.5\tan^{-1}\{(\sqrt{\{s_2(n)\}^2 + \{s_3(n)\}^2})/s_1(n)\}$ and $\tan^{-1}(s_3(n)/s_2(n))$ respectively. Herein, each signal at two orthogonal polarization axes suffers almost the same SOP variation, which consisted of same $\alpha(n)$ and $\Delta\beta(n)$. It is because polarization mode dispersion between two orthogonal axes is too small in the standard C-band SSMF as demonstrated in [22]. Each SV index is defined as:

$$\begin{aligned} SV(n) &= [s_1(n);\ s_2(n);\ s_3(n)] \\ &= \left[A_x^2 - A_y^2;\ 2A_xA_y\cos(\theta_{x_0} - \theta_{y_0});\ 2A_xA_y\sin(\theta_{x_0} - \theta_{y_0})\right]. \end{aligned} \tag{2-2}$$

Herein, the reason why we use SV expression in Eq. (2) is that it uses the amplitudes and relative phase difference of both polarization axes without any PN information. It can also represent SOP of light in three dimensions-based Poincare sphere more accurately than two dimensions-based Jones vector's one as compared in [17].

In Eq. (2), $CPE_{n,k}$, and $major - ICI_{n,k}$ indicate the SOP variation during transmission in [12], CPE $(=\exp(j\theta_{r_{n,k}})$, where $\theta_{r_{n,k}}$ means rotated angle due to CPE of the n-*th* frame and the k-*th* subcarrier) and major-ICI term. Herein, major-ICI term at the k-th DPC-PT as follows:

$$\begin{aligned} major - ICI_{n,k} &= S_{n,k-1} \cdot I(n,1) + S_{n,k+1} \cdot I(n,-1), \\ where\ ICI_{n,k} &= \sum_{l=0, l\neq k}^{K-1} S_{n,l} \cdot I(n, k-l) \\ and\ I(n,k) &= \frac{1}{K} \sum_{a=0}^{K-1} \exp\{j2\pi ka/K + j\theta_{r_{n,a}}\}. \end{aligned} \tag{2-3}$$

In Eq. (2-3), among total ICI terms of $1{\sim}K$-*th* subcarrier as derived in [23], in this paper, only ICI term from adjacent two PTs are considered and it is so-called major-ICI term. Another ICI term is ignored due to small noise power at k-*th* DPC-PT [24], [25]. For instance, at k-*th* DPC-PT, major-ICI term is related to the adjacent subcarriers of left ($(k-1)$-*th*) and right ($(k+1)$-*th*) side. In Eq. (2) including both MNs, multiple SOPLs due to $M_p(n)$ can degrade the SNR at the reference polarization axis, whereas multiple PNs can rotate the phase of the symbol in both in-phase and quadrature (I/Q) axes. Herein, the important point is that adjacent OFDM subcarriers undergo a similar channel response due to their narrow subchannel spacing; i.e., both MNs are almost the same between a pair of DPC-PTs. By using this important property, both MNs can be tracked as followed steps.

The third step is the SOPL tracking within one ONU whose signal is separated in the second step for parallel processing. In this step, $M_p(n)$ can be estimated by comparing transmitted/received DPC-PTs. Each averaged value of both transmitted and received DPC-PTs in the time domain, which are tten as $pr(n)$ *and* $ps(n)$ respectively, can be expressed as:

$$\begin{aligned} pr(n) &= (R_{n,k} + R_{n,k+1})/2 \\ &= M_p(n) \begin{bmatrix} A_x\cos(\theta_{x_0}) \cdot CPE_{n,k} + W_{n,k} \\ A_y\cos(\theta_{y_0}) \cdot CPE_{n,k} + W_{n,k} \end{bmatrix} \\ ps(n) &= (S_{n,k} + S_{n,k+1})/2 = \left[A_x\cos(\theta_{x_0});\ \ A_y\cos(\theta_{y_0})\right], \end{aligned} \tag{3}$$

where $W_{n,k}$ denotes arithmetic mean value of k- and $(k+1)$-*th* subcarriers' major- ICI at each polarization axis. Eq. (3) can be transposed to two SVs: $SV_{pr}(n)$ *and* $SV_{ps}(n)$ by using Eq. (2-2). Since these vectors have no relationship to the PNs [17], we can focus on SOPLs only in this step. Then, both SVs are compared in Poincare sphere, which consisted of three-dimensional spherical coordinates such as $(s_1(n), s_2(n), s_3(n))$. By comparing both points of SVs, we can calculate $M_p(n)$ because it consisted of SVs as shown

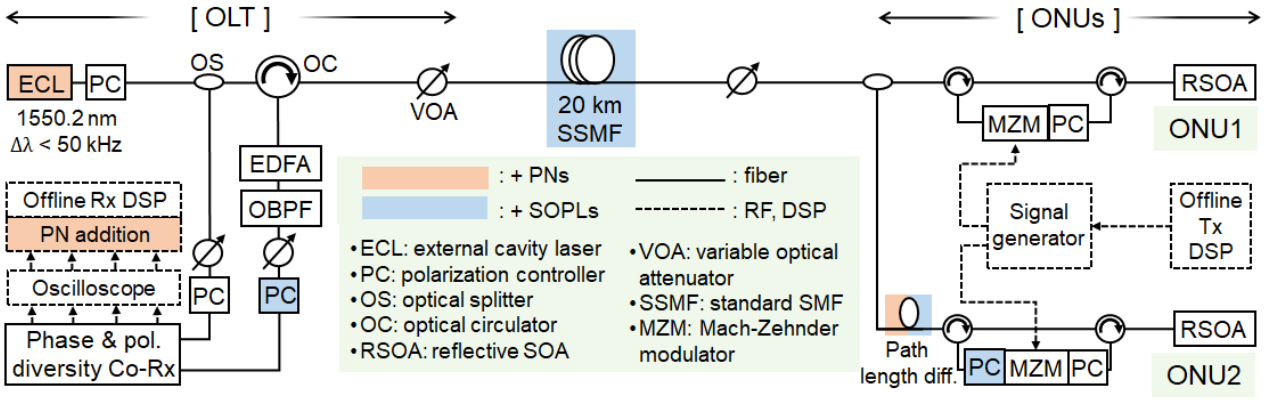

FIGURE 3. Experimental setup for verification of the proposed technique.

in both Fig. 2 and Eq. (2-1). Additionally, the tracking accuracy can be improved compared with the previous single PT-based technique [12] because of the doubled estimator sample number. By tracking SOP matrix and multiplying $M_p^{-1}(n)$ to the received signal, a compensated signal $\overline{S_{n,K}}$ can be obtained:

$$\overline{S_{n,K}} = M_p^{-1}(n)R_{n,K} = \begin{bmatrix} CPE_{n,K} \cdot E_{x_{n,K}} + major - ICI_{n,K} \\ CPE_{n,K} \cdot E_{y_{n,K}} + major - ICI_{n,K} \end{bmatrix}. \tag{4}$$

Then, the last step is progressed after FFT for phase tracking by averaging a pair of DPC-PTs as follows:

$$\begin{aligned} &(\overline{S_{n,k}} + \overline{S^*_{n,k+1}})/2 \\ &= \{CPE_{n,k}S_{n,k} + CPE^*_{n,k}S_{n,k} \\ &\quad + S_{n,k+1}I(n,-1) + S^*_{n,k}I^*(n,1) + S^*_{n,k+2}I^*(n,-1)\}/2 \\ &= [2S_{n,k}\cos\theta_{r_{n,k}} + S_{n,k-1}I(n,1) + S^*_{n,k+2}I^*(n,-1) \\ &\quad + S_{n,k+1}\frac{1}{K}\sum_{a=0}^{K-1}\{2\exp(-j2\pi ka/K)\cos(\theta_{r_{n,a}})\}]/2. \end{aligned} \tag{5}$$

When CPE is tracked, major-ICI level can affect tracking accuracy because this level acts as a noise level. It is a well-known fact that estimation accuracy is directly related to the noise level. If we use conjugated PTs as derived in Eq. (5), major-ICI level can be partially reduced compared to the non-conjugated PTs-based tracking. In Eq. (5), the amplitude of partial major-ICI $(S_{n,k+1}\frac{1}{K}\sum_{a=0}^{K-1}\{2\exp(-j2\pi ka/K)\cos(\theta_{r_{n,a}})\})$ can be reduced, where $|\cos(\theta_{r_{n,a}})| \leq 1$. If $|\cos(\theta_{r_{n,a}})|$ equals to *0*, maximally up to 50 % of the major-ICI level can be reduced. This ICI reduction effect is as similar as two subcarriers are used in [23]. On the other hand, in the non-conjugate case, the same component is represented as an exponential term whose maximum amplitude is bigger than the conjugate case due to $|\exp(j\theta_{r_{n,a}})| \leq \sqrt{2}$. Due to retaining SNR relatively, CPE can be extracted more clearly. Further, this advantage significantly works in high-order modulation or narrow sub-channel spacing-based CO-OFDM transmission due to a higher ICI level. By comparing averaged transmitted/received DPC-PTs, CPE can be estimated:

$$\theta_{r_{n,k}} = \arg\{\frac{(\overline{S_{n,k}} + \overline{S^*_{n,k+1}})/2}{(S_{n,k} + S^*_{n,k+1})/2}\}. \tag{6}$$

In Eq. (6), $\arg(x)$ denotes the argument function, which is a phase value of x. Herein, CPE can be estimated and abbreviated to cosine terms. The inverse value of CPE is multiplied to all subcarriers. Finally, a recovered signal can be written as follows:

$$\widetilde{S_{n,K}} = \exp(-\theta_{r_{n,k}})\overline{S_{n,K}}. \tag{7}$$

Then, the conventional channel equalization and demodulation process can be conducted. The values of estimated MNs are updated by every frame and the update period can also be adjusted. Besides, the proposed technique can be easily applied to the conventional MQAM-OFDMA system. The most important advantage is to track both MNs with the same estimator and separately per ONU in the multiple-access Thus, each ONU does not require any other optical polarization and phase controlling for parallel MNs handling.

III. EXPERIMENTAL VERIFICATION

Figure 3 shows the experimental setup. This experiment aimed to compensate MNs by using the proposed technique in the conventional MQAM-based CO-OFDMA-PON uplink transmission. Even though the proposed technique could be applied to both phase and polarization diversity-based system, the single wavelength-based CO-OFDMA-PON with single-polarization was used as a proof-of-concept of verification for DPC-PTs-based tracking. For verification, the structure of an optical carrier-suppressed self-coherent reflective PON (OCS-SCR-PON) was used as a basic scheme.

A. TARGET CO-PON MULTIPLE ACCESS OPTICAL LINK FOR VERIFICATION: OPTICAL CARRIER-SUPPRESSED SELF-COHERENT REFLECTIVE PON

In this experiment, a SCR-PON system was used as a basic transmission structure. Basic SCR-PON structure consisted of self-coherent-based OLT and reflective ONU [26]. The self-coherent means self-homodyne detection. Self-homodyne detection uses the same optical source for both signal and local oscillator (LO) sources. It can be realized by sharing the optical laser source (for signal modulation) as a LO also. Laser source for LO for coherent detection can be replaced by using partial optical seed source for ONU. In Fig. 3, optical seed source for ONU can be split into two optical paths by an optical splitter. Between two paths, one is used for self-homodyne reception, and the other one goes through the ONU side for uplink signal modulation. Reflective ONU means to distribute the optical source for uplink transmission from the OLT side by using the reflective optical components such as a reflective semiconductor optical amplifier (RSOA), reflective electro-absorption modulator, and so on as summarized in [26]. To generate the unmodulated uplink wavelengths at the OLT side, reflective-type optical components such as reflective optical amplifier or reflective modulator can be used. After reflection of the seed source, which comes from OLT side, we can modulate uplink signal by using this reflected optical carrier at ONU side. If RSOA, which combines both amplifier and modulator within single device, is used as a reflective ONU [27], [28], this structure can secure optical power margin for uplink transmission due to its' optical gain. In addition, by replacing laser source for each ONU as a reflective component, the cost and complexity of the ONU side are significantly reduced and colorless operation for WDM can be ensured also. Above all, there were no multiple carrier frequency offsets because the same optical seed source was shared per ONU.

On the other hand, optical-beat-interference (OBI) and carrier-induced Rayleigh back-scattering (RBS), as well as both multiple SOPLs and PNs, could affect the uplink signal [27]–[29]. The optical carrier from multiple-ONUs and LO carrier could interfere with each other due to square-law detection by a PD. Further, fiber non-uniformity could cause RBS. Both problems could degrade transmission performance, so they needed to be solved before performing this experiment. In our previous work [12], [13], [27], [28], a simple optical carrier suppression technique was studied to find out a way of mitigating unwanted OBI and carrier-induced RBS noises. As a result, we had to focus on multiple SOPLs and PNs issues in OCS-SCR-PON multiple access situations.

B. PARAMETER SETTINGS FOR TRANSMISSION

In Fig. 3, an uplink transmission with two ONUs was assumed. Herein, two signals of both ONUs were simultaneously transmitted to the OLT. In the OLT, an external cavity laser (ECL: center wavelength: 1550.2 nm and linewidth $<$50 kHz) was divided into two paths by an optical splitter. Each half was used as the optical source to seed for ONUs and to the LO for the OLT. To exclude the fiber nonlinearity, the initial optical power of the seed source was a low power of -5 dBm. Then, its initial SOP was aligned by a fiber squeeze-type polarization controller (PC). This source passed through the standard C-band SMF and reached into two ONUs whose optical power was each -13 dBm. At each ONU, the seed source was reflected and amplified up to $+4$ dBm using the RSOA. The amplified source was connected to the Mach-Zehnder modulator (MZM) to modulate the uplink signal. The real-valued 16QAM-OFDMA signal of each ONU was generated by a signal generator. The real-valued OFDMA signal was generated using Hermitian symmetry during the IFFT process for optical intensity modulator [8], [30]. The uplink signal was converted to the optical signal using MZM, where the electrical bias was set at the null-point to suppress OBI and carrier-induced RBS [12], [13], [27]–[31]. Each modulated signal was combined using an optical combiner and transmitted to 20-km SSMF, where the PMD could be ignored [22]. After the in-line implication of the received signal, the OLT self-coherently received it with the phase and polarization diversity based coherent receiver (Fujitsu, FIM 24706: 100 Gbps Dual-polarization quadrature phase shift keying receiver). The receiver sensitivity was -36 dBm at the on-off keying of 6 GHz back-to-back (BtB) transmission with the target BER of 2×10^{-3} to satisfy the forward error correction (FEC) limit. Then, the received signal was captured using an oscilloscope whose sampling rate was 50G samples/sec. At DSP part, 16QAM-OFDMA signal of 3 GHz with DPC-PTs per ONU (ONU1: 0-3 GHz, ONU2: 3-6 GHz) was implemented. The DPC-PTs were assigned to the middle point of each ONU band (about 1.5 and 4.5 GHz per ONU) to guarantee sufficient SNR except at the boundary of each band. A guard-band was designed by nulling one subcarrier at the boundary of each band. Since each uplink signal was asynchronously transmitted, a cyclic prefix (CP) with a length of 5 % of the OFDMA symbol duration was inserted and the total sample was oversampled by a factor of 2.

C. PARAMETER SETTING FOR MNS GENERATION

To evaluate the effectiveness of the proposed technique, the transmission performance was examined in the presence of both MNs. For multiple PNs generation, an artificial PN addition block was added before Rx DSP. The DSP block based on the Wiener PN model was inserted to observe the PN effect as a function of the laser linewidth [14]. Even though each ONU shared the same optical source, we emulated different multiple PNs by making an optical path difference between two ONUs. For multiple SOPLs generations, different polarization-sensitive optical amplifiers, MZMs, and optical attenuators were used for each ONUs. Initial SOPs of both ONUs were fixed to X-polarization (0° linear polarization) by using a PC before each MZM as shown in Fig. 2. Two PCs after MZM of ONU2 and before Co-Rx were used for different SOPLs generation.

IV. RESULTS AND DISCUSSION

In this section, we discuss the compensation effects of the DPC-PTs-based compensation technique. First, multiple SOPLs compensation was verified with a small multiple PNs effect. Second, multiple PNs compensations was performed with the minimized multiple SOPLs. Third, the transmission performance was evaluated in the presence of both MNs. Last, a comparison of the proposed technique with a conventional PT-based technique was examined, and the number of DPC-PTs was optimized in the given transmission condition.

A. SOPLs COMPENSATION

Figure 4 shows the compensation effect of multiple SOPLs. The RMSE in the Poincare sphere was measured by changing the optical splitting power. The condition of a linewidth of 50 kHz, 256 subcarriers, and initial SOP of x-polarization was assumed. Herein, the multiple PNs effect was too small because of a narrow laser linewidth to enable us to focus on the multiple SOPLs. At the optical back-to-back (BtB) transmission, the initial SOP could not be maintained because of polarization-sensitive devices. Moreover, this SOP was more scattered in the Poincare sphere in 20-km transmission because of the birefringence property of SSMF. For both transmission distances, SNR at the reference polarization axis (x-polarization axis) was lowered owing to multiple SOPLs for the undesired polarization axis (y-polarization axis). Since SOP changed according to both devices and path length difference per ONU, it was estimated independently in the Poincare sphere after ONU extraction. RMSE could be successfully mitigated due to SOPLs correction. This was done through the use of superposed components between two DPC-PTs. Even if the number of ONUs (splitting ratio) was increased, a successful and parallel SOPL handling was possible. About 8.48 % and 28.63 % of RMSE were improved in BtB and 20-km cases respectively. For a high splitting ratio of more than 1:512 at 20-km, the degree of EVM improvement was decreased because of low SNR and an insufficient number of DPC-PTs. However, this limitation could be improved by using additional SNR securing techniques. An important point of Fig. 4 was that the SV-based multiple SOPLs compensations worked well in the presence of multiple SOPLs supporting 256 subscribers. This was because the SV did not care about the linewidth of the laser source, where the small multiple PNs existed.

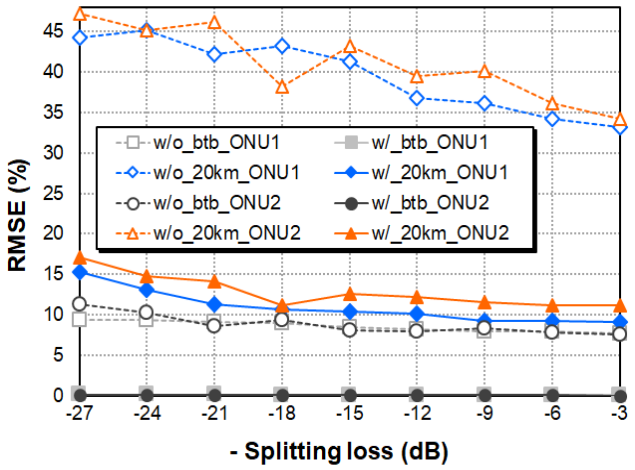

FIGURE 4. RMSE for according to splitting loss, where initial SOP was X-polarization (SV = (1, 0, 0)).

B. PNs COMPENSATION

Figure 5 (a) shows the EVM performance according to the total linewidth (50 kHz of ECL + additional linewidth of PN addition DSP block). To focus on the multiple PNs, BtB transmission was assumed with the minimum SOP variation. Instead of using lasers with various linewidths, a DSP-based PN addition function was inserted. The purpose of this experiment was to examine the effects of multiple PNs with respect to the laser linewidth and to verify the proposed technique in the OCS-SCR-PON multiple access. Since multiple PNs got worse in proportion with the laser linewidth, the EVM became degraded and the signal could not be demodulated normally. Each OFDMA subcarriers of both ONUs provided poor quality of uplink service. The uplink transmission performance became severe and we could not recover the transmitted data in higher-order-based QAM-OFDMA transmission. As the inter-symbol distance became narrower, it would be more sensitive to the interference. In addition, these PNs per ONU were slightly different owing to the different optical

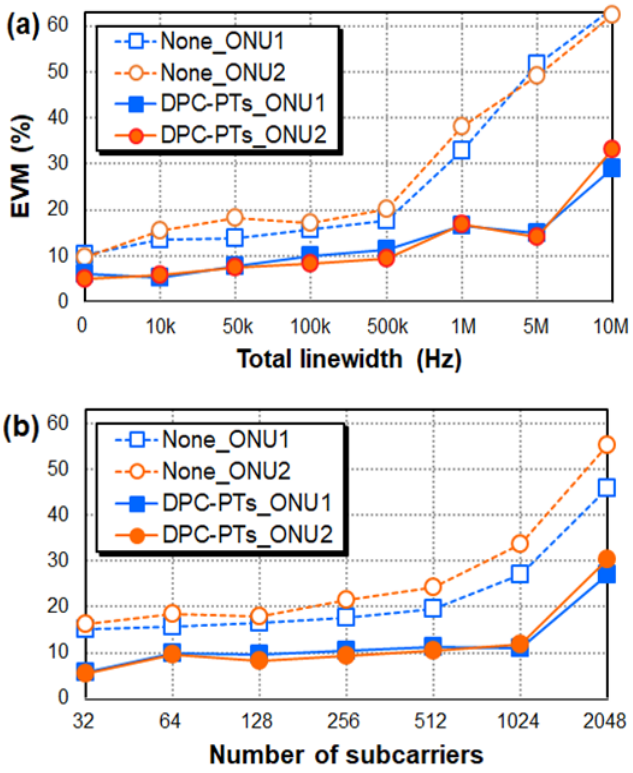

FIGURE 5. EVM according to the (a) total linewidth which is the sum of the linewidth of ECL and PN addition and (b) subcarrier numbers.

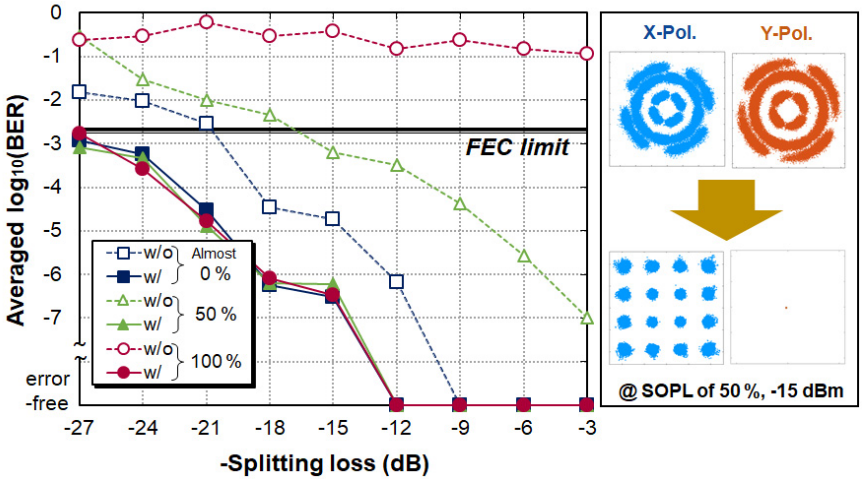

FIGURE 6. Averaged BER performance according to the splitting ratio in the presence of both MNs and constellation diagrams.

path length on each ONU side. In contrast, by applying the DPC-PTs based technique in this situation, the EVMs of both ONUs were improved by using the phase-conjugated estimators; for instance, an EVM improvement of 7.87 % could be achieved in the total linewidth of 500 kHz.

Figure 5 (b) shows the plotted EVM performance according to the 16QAM-OFDMA subchannel spacing when the total linewidth was fixed to 500 kHz. In the given OCS-SCR-PON structure, the EVM performance could be different even though the linewidths of both ONUs were the same. In each ONU, even with the fixed laser linewidth, the effect of the multiple PNs could be stronger as the subchannel spacing became narrower. This was because a narrower subchannel spacing made each subcarrier more sensitive to both CPE and ICI components. In addition, there was a slight optical path length difference between the two ONUs, and each ONU suffered from a different PN. With the proposed technique, when 256 subcarriers were used (subchannel spacing was about 5 MHz), EVM was improved up to 5.44 %. As a result, parallel PNs tracking verified by using a pair of DPC-PTs per ONU. As a result of both Figs. 5 (a) and (b), the proposed technique enabled independent and accurate multiple PNs compensation by multiple-accessed ONUs in the presence of severe multiple PNs.

C. BOTH SOPLs AND PNs COMPENSATION

In a practical uplink transmission environment with multiple-accessed ONUs, both MNs can be simultaneously generated. Thus, SSMF transmission performance in the presence of both MNs should be compared to evaluate the effect of the proposed technique. With fixed linewidth of 500 kHz and transmission distance of 20-km, the averaged BER performance between two ONUs was measured as shown in Figure 6. The target BER was set to 2×10^{-3} to satisfy the FEC limit. The averaged BER performance was measured for three SOPL cases, as mentioned in Section III. In ideal multiple SOPLs case (almost 0 % of SOPLs) despite of the fixed initial SOPs at each transmitter, the received SOPs could not be maintained because of the signal leakage to the undesired y-polarization axis. In addition, the received 16 QAM-OFDMA signal at the reference x- polarization axis could be rotated in I/Q domains with respect to multiple PNs as shown in constellation diagrams. Both MNs should be solved to secure sufficient BER for the FEC limit. In both orthogonal and worst SOPL cases (50 % and 100 % SOPLs respectively), the mean BER performance got worse because the SNR became lower at the reference polarization axis. Additionally, multiple PNs could deteriorate the received symbols more seriously. On the other hand, the proposed technique allowed us to achieve BER under FEC limit for all SOPLs cases. This was because the undesired multiple SOPLs were corrected to the reference polarization axis and the multiple PNs were compensated through the DPC-PTs. In constellation diagrams, a clear correction of both MNs could be measured. Supporting up to 256 ONUs (splitting loss = 24 dB) was enabled in 20-km SSMF uplink transmission under the FEC limit. Consequently, lots of ONUs could have stable optical access through the proposed technique.

D. OPTIMIZATION OF THE NUMBER OF DPC-PTs

In Figure 7, the overhead due to the number of PTs and mean EVM performance are presented. The given transmission conditions were as follows: a total linewidth of 500 kHz, 20 km SSMF transmission, 50 % SOPLs case. As the number of PTs per ONU increased, the mean EVM was improved because more accurate MNs estimation was possible due to the increased sample numbers of the estimator. But it was saturated after eight numbers of PTs because our proposed technique did not handle another noise component such as amplified spontaneous emission noise. Nevertheless, the reason why conjugated PTs were used was that more accurate CPE tracking was possible due to retained SNR between

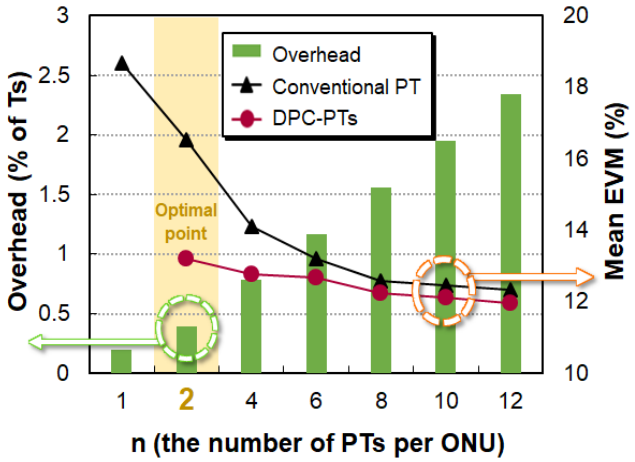

FIGURE 7. Overhead and mean EVM according to the number of PTs.

estimators compared to the non-conjugated PT-based tracking. If a pair of DPC-PTs was used, about EVM of 3.32 % was improved compared to the non-conjugated PTs-based tracking. Important point was to maximize the transmission performance with the minimum overhead of DPC-PTs under the target BER performance. Herein, the minimum overhead due to a pair of DPC-PTs within unit *Ts* while satisfying the target BER under the given transmission condition was 0.39 %. If the transmission condition is changed, the total number of DPC-PTs needs to be re-optimized.

V. CONCLUSION

In summary, this study proposed the simple and effective solution for MNs in the conventional MQAM-based CO-OFDMA-PON system using DPC-PTs. By using two conjugated PTs, both noise components could be extracted with the same estimator per ONU. MNs compensation was possible in experimental verification by achieving multiple SOPLs corrections in the Poincare sphere and multiple PNs compensation. In addition, a smaller number of redundant subcarriers were verified for offering the highest transmission performance. Consequently, the proposed technique worked in the presence of severe MNs without increasing optical transmission system complexity. By using the proposed technique, it is expected that providing a stable uplink transmission service is possible in another system utilizing both phase and polarization diversities as well as a single wavelength-based CO-OFDMA-PON uplink transmission, which was we have emulated, by using the proposed tracking technique. Furthermore, the proposed technique could deliver high-quality service in case of future optical access networks for more massive subscribers.

REFERENCES

[1] R. Koma, "Standardization trends for future high-speed passive optical networks," *NTT Tech. Rev.*, vol. 15, no. 10, pp. 1–5, Oct. 2017.
[2] F. Halabi, L. Chen, R. P. Giddings, A. Hamie, and J. M. Tang, "Multilevel subcarrier index-power modulated optical OFDM with adaptive bit loading for IMDD PON systems," *IEEE Photon. J.*, vol. 8, no. 6, Dec. 2016, Art. no. 7907114.
[3] S.-Y. Jung, S.-M. Jung, and S.-K. Han, "I/Q channel separated baseband OFDM optical transmission using orthogonal polarizations in IM/DD system," *J. Lightw. Technol.*, vol. 32, no. 13, pp. 2392–2398, Jul. 2014.
[4] R. Ullah, L. Bo, S. Ullah, M. Yaya, F. Tian, M. K. Khan, and X. Xiangjun, "Flattened optical multicarrier generation technique for optical line terminal side in next generation WDM-PON supporting high data rate transmission," *IEEE Access*, vol. 6, pp. 6183–6193, 2018.
[5] R. Ullah, L. Bo, S. Ullah, M. Yaya, F. Tian, and X. Xiangjun, "Cost effective OLT designed from optical frequency comb generator based EML for1.22 Tbps wavelength division multiplexed passive optical network," *Opt. Fiber Technol.*, vol. 43, pp. 49–56, Jul. 2018.
[6] K. Kikuchi, "Fundamentals of coherent optical fiber communications," *J. Lightw. Technol.*, vol. 34, no. 1, pp. 157–179, Jan. 2016.
[7] N. Suzuki, H. Miura, K. Matsuda, R. Matsumoto, and K. Motoshima, "100 Gb/s to 1 Tb/s based coherent passive optical network technology," *J. Lightw. Technol.*, vol. 36, no. 8, pp. 1485–1491, Apr. 2018.
[8] W. Shieh and I. Djordjevic, *Orthogonal Frequency Division Multiplexing for Optical Communications*, 1st ed. Amsterdam, The Netherlands: Elsevie, 2010, pp. 127–138.
[9] S.-M. Kang, C.-H. Kim, S.-M. Jung, and S.-K. Han, "Timing-offset-tolerant universal-filtered multicarrier passive optical network for asynchronous multiservices-over-fiber," *J. Opt. Commun. Netw.*, vol. 8, no. 4, pp. 229–237, Apr. 2016.
[10] C. Li, "4×128-Gb/s PDM-DMT signal transmission over 1440-km SSMF with high phase noise tolerance," *Opt. Express*, vol. 26, no. 23, pp. 30901–30909, Nov. 2018.
[11] S.-M. Jung, K.-H. Mun, S.-Y. Jung, and S.-K. Han, "Optical-beat-induced multi-user-interference reduction in single wavelength OFDMA PON upstream multiple access systems with self-homodyne coherent detection," *J. Lightw. Technol.*, vol. 34, no. 11, pp. 2804–2811, Jun. 2016.
[12] S.-M. Kang, K.-H. Mun, H.-J. Park, and S.-K. Han, "Individual Stokes-vector-based SOP recovery in CO-OFDMA-PON uplink transmission," *IEEE Photon. Technol. Lett.*, vol. 30, no. 9, pp. 829–832, May 1, 2018.
[13] K.-H. Mun, S.-M. Kang, and S.-K. Han, "Multiple-noise-tolerant CO-OFDMA-PON uplink multiple access using AM-DAPSK-OFDM with reflective ONUs," *J. Lightw. Technol.*, vol. 36, no. 23, pp. 5462–5469, Dec. 2018.
[14] L. Tomba, "On the effect of wiener phase noise in OFDM systems," *IEEE Trans. Commun.*, vol. 46, no. 5, pp. 580–583, May 1998.
[15] H. K. Shim, K. Y. Cho, U. H. Hong, and Y. C. Chung, "Transmission of 40-Gb/s QPSK upstream signal in RSOA-based coherent WDM PON using offset PDM technique," *Opt. Express*, vol. 21, no. 3, p. 3721, Feb. 2013.
[16] J. Fatome, "A universal optical all-fiber omnipolarizer," *Sci. Rep.*, vol. 2, pp. 938–946, Dec. 2012.
[17] B. Szafraniec, B. Nebendahl, and T. Marshall, "Polarization demultiplexing in Stokes space," *Opt. Express*, vol. 18, no. 17, p. 17928, Aug. 2010.
[18] T. Ye, "A polarization change monitor by eigenvalue analysis in coherent receiver," in *Proc. OFC*, Los Angeles, CA, USA, 2019, Paper M4I.1.
[19] C. Xie and G. Raybon, "Digital PLL based frequency offset compensation and carrier phase estimation for 16QAM coherent optical communication systems," in *Proc. ECOC*, Amsterdam, The Netherlands, 2012, Paper Mo.1.A.2.
[20] S. Cao, P. Yuen Kam, and C. Yu, "Decision-aided, pilot-aided, decision-feedback phase estimation for coherent optical OFDM systems," *IEEE Photon. Technol. Lett.*, vol. 24, no. 22, pp. 2067–2069, Nov. 15, 2012.
[21] S. Moriyama, K. Tsuchida, and M. Sasaki, "Digital transmission of high bit rate signals using 16DAPSK-OFDM modulation scheme," *IEEE Trans. Broadcast.*, vol. 44, no. 1, pp. 115–122, Mar. 1998.
[22] N. J. Muga and A. N. Pinto, "PMD tolerance in Stokes space based polarization de-multiplexing algorithms," *Opt. Quant. Electron.*, vol. 49, no. 6, pp. 1–10, 2017.
[23] X. Yi, B. Xu, J. Zhang, Y. Lin, and K. Qiu, "Theoretical calculation on ICI reduction using digital coherent superposition of optical OFDM subcarrier pairs in the presence of laser phase noise," *Opt. Express*, vol. 22, no. 25, Dec. 2014, Art. no. 31192.
[24] S. William and I. Djordjevic, *OFDM for Optical Communications: Chapter 2: OFDM Principles*. New York, NY, USA: Academic, 2009, pp. 31–52.
[25] P. Robertson and S. Kaiser, "Analysis of the effects of phase-noise in orthogonal frequency division multiplex (OFDM) systems," in *Proc. IEEE Int. Conf. Commun. (ICC)*, vol. 3, Nov. 2002, pp. 1652–1657.

[26] M. Yasin, H. Arof, and S. Harun, "Self-coherent reflective passive optical networks," in *Advances in Optical Fiber Technology: Fundamental Optical Phenomena and Applications*. Rijeka, Croatia: InTech, Feb. 2015, pp. 365–386.
[27] S.-M. Kang, K.-H. Mun, S.-M. Jung, and S.-K. Han, "Mitigation of optical interference noise by optical carrier cancelation in self-coherent reflective PON uplink transmission," *IEEE Photon. J.*, vol. 9, no. 3, Jun. 2017, Art. no. 7903509.
[28] S.-M. Jung, K.-H. Mun, S.-M. Kang, and S.-K. Han, "Carrier-suppressed reflective coherent passive optical network uplink transmission for optical interference mitigation," in *Proc. 19th Int. Conf. Transparent Opt. Netw. (ICTON)*, Jul. 2017, Paper Tu.C2.6.
[29] S. Abrate, S. Straullu, A. Nespola, P. Savio, J. Chang, V. Ferrero, B. Charbonnier, and R. Gaudino, "Overview of the FABULOUS EU Project: Final system performance assessment with discrete components," *J. Lightw. Technol.*, vol. 34, no. 2, pp. 798–804, Jan. 15, 2016.
[30] N. Cvijetic, D. Qian, J. Hu, and T. Wang, "Orthogonal frequency division multiple access PON (OFDMA-PON) for colorless upstream transmission beyond 10 Gb/s," *IEEE J. Sel. Areas Commun.*, vol. 28, no. 6, pp. 781–790, Aug. 2010.
[31] N. Cvijetic, "OFDM for next-generation optical access networks," *J. Lightw. Technol.*, vol. 30, no. 4, pp. 384–398, Feb. 15, 2012.

SOO-MIN KANG received the B.S. degree in electronic engineering from Sogang University, Seoul, South Korea, in 2014, and the M.S. degree in electrical and electronic engineering from Yonsei University, Seoul, in 2016, where she is currently pursuing the Ph.D. degree in electrical and electronic engineering. Her current research interests include coherent optical access networks, passive optical networks, and software-defined optical networks.

HYOUNG JOON PARK received the B.S. and M.S. degrees in electronic engineering from Yonsei University, Seoul, South Korea, in 2014 and 2016, respectively, where he is currently pursuing the Ph.D. degree in electrical and electronic engineering. His current research interests include multidimensional optical transmission, OFDMA-PON, and next-generation access networks.

INHO HA received the B.S. and M.S. degrees in electronic engineering from Yonsei University, Seoul, South Korea, in 2017 and 2019, respectively, where he is currently pursuing the Ph.D. degree in electrical and electronic engineering. His research interests include wireless/wireline convergence and next-generation mobile front haul.

SANG-KOOK HAN (Senior Member, IEEE) received the B.S. degree in electronic engineering from Yonsei University, Seoul, South Korea, in 1986, and the M.S. and Ph.D. degrees in electrical engineering from the University of Florida, Gainesville, FL, USA, in 1994. From 1994 to 1996, he was with the System IC Laboratory, Hyundai Electronics, where he was involved in the development of optical devices for telecommunications. He is currently a Professor with the Department of Electrical and Electronic Engineering, Yonsei University. His current research interests include optical devices/systems for communications, optical OFDM transmission systems, passive optical networks, optical networks, and visible-light communication technologies.